The acceleration of oceanic denitrification during deglacial warming

NICOPP working group members[†]

Over much of the ocean's surface, productivity and growth is limited by a scarcity of bioavailable nitrogen. Sedimentary $\delta^{15}N$ records spanning the last deglaciation suggest marked shifts in the nitrogen cycle during this time, but the quantification of these changes has been hindered by the complexity of nitrogen isotope cycling. Here we present a database of $\delta^{15}N$ in sediments throughout the world's oceans, including >2,300 modern seafloor samples, and 76 timeseries spanning the past 30,000 years. We show that the $\delta^{15}N$ values of modern seafloor sediments are consistent with values predicted by our knowledge of nitrogen cycling in the water column. Despite many local deglacial changes, the globally averaged $\delta^{15}N$ values of sinking organic matter were similar during the Last Glacial Maximum and Early Holocene. Considering the global isotopic mass balance, we explain these observations with the following deglacial history of nitrogen inventory processes. During the Last Glacial Maximum, the nitrogen cycle was near steady state. During the deglaciation, denitrification in the pelagic water column accelerated. The flooding of continental shelves subsequently increased denitrification at the seafloor, and denitrification reached near steady-state conditions again in the Early Holocene. We use a recent parameterization of seafloor denitrification to estimate a 30–120% increase in benthic denitrification between 15,000 and 8,000 years ago. Based on the similarity of globally averaged $\delta^{15}N$ values during the Last Glacial Maximum and Early Holocene, we infer that pelagic denitrification must have increased by a similar amount between the two steady states.

N itrogen is a critical component of all living matter. But despite the ubiquity of dissolved N_2 gas in the ocean, its bioavailable forms (N_{bio}, most of which is NO_3^-) are scarce in the sunlit surface layer, and its limited supply exerts the primary nutritional constraint on the marine ecosystem. Within the oceans, N_2 is fixed to N_{bio} almost entirely by micro-organisms near the ocean surface, and returned to N_2 by denitrification (including anammox) in suboxic zones of the water column and sediment, turning over the N_{bio} inventory on a timescale of ~3 kyr (ref. 1). The nitrogen cycle can alter the radiative properties of the atmosphere, through the generation of N_2O (ref. 2) and by supporting the biological sequestration of CO_2 in the ocean[3,4].

Humans are transforming the nitrogen cycle by approximately doubling the pre-industrial rate of terrestrial N_2 fixation and by supplying N_{bio} to the ocean surface through rivers and the atmosphere[1]. Meanwhile, anthropogenic warming is expected to increase the rate of denitrification, by expanding water column oxygen minimum zones[1,5], and to also modify the supply routes of nitrate by changing ocean circulation[6]. However, the observational record of oceanic nitrate concentrations is much shorter than the residence time of N_{bio} and is barely able to resolve decadal fluctuations in nitrate availability[7], preventing the identification of climatic trends.

In contrast, the geological record spans vast timescales and documents large climate shifts, such as the glacial/interglacial cycles. The nitrogen stable isotope ratio ($\delta^{15}N = {}^{15}N/{}^{14}N_{sample}/{}^{15}N/{}^{14}N_{ref} - 1) * 1,000‰$) of sinking organic matter is preserved in marine sediments[8], providing a window on past changes in the nitrogen cycle. Over recent decades, an understanding of nitrogen isotope systematics has developed from field and laboratory studies, and nitrogen isotope records have been generated from seafloor sediments extending back thousands (or in some cases millions) of years. The sedimentary record of the last ice age cycle is par-

ticularly well sampled, and has revealed signs that pelagic denitrification was less active during cold periods[3,9]. Meanwhile, the subaerial exposure of continental shelves during glacial sea-level low-stands would have eliminated the most active regions of benthic denitrification[10], leading to a further reduction in the loss rate of N_{bio}. Efforts to reconstruct past denitrification rates have, to date, proceeded piecemeal, focusing on small numbers of records. Here we present the first global analysis of available $\delta^{15}N$ observations, starting with a synoptic picture of the present day seafloor, and proceeding to a quantitative analysis of the last deglaciation.

A synoptic view of N isotopes in the modern ocean

The $\delta^{15}N$ of organic matter at the ocean surface depends on two factors: the global mean $\delta^{15}N$ of N_{bio} ($\delta^{15}N_{mean}$, currently ~5‰), and the differential distribution of ^{14}N and ^{15}N within the ocean. The relative rates of N_2 fixation and denitrification are the primary controls on $\delta^{15}N_{mean}$ (ref. 11, Fig. 1), and alter the distribution of $\delta^{15}N$ by imprinting their isotopic signatures where they are most intense. Meanwhile, the preferential partitioning of ^{14}N into sinking organic particles by the marine ecosystem conspires with ocean circulation to produce a second, more subtle class of isotopic redistribution. We refer to these as 'inventory-altering' and 'internal-cycling' fractionation processes, respectively (see Supplementary Information for more information). The sinking of particulate organic matter transfers the isotopic signature of surface ocean nitrogen to the seafloor[8,12].

Figure 2a shows our compilation of >1,500 measurements of the $\delta^{15}N$ of total combustible (bulk) nitrogen at the modern seafloor. These measurements show good lateral continuity in most parts of the ocean, with strong gradients generally occurring in regions with strong oceanographic fronts[13]. Some aspects of the large-scale patterns correspond directly to the distribution

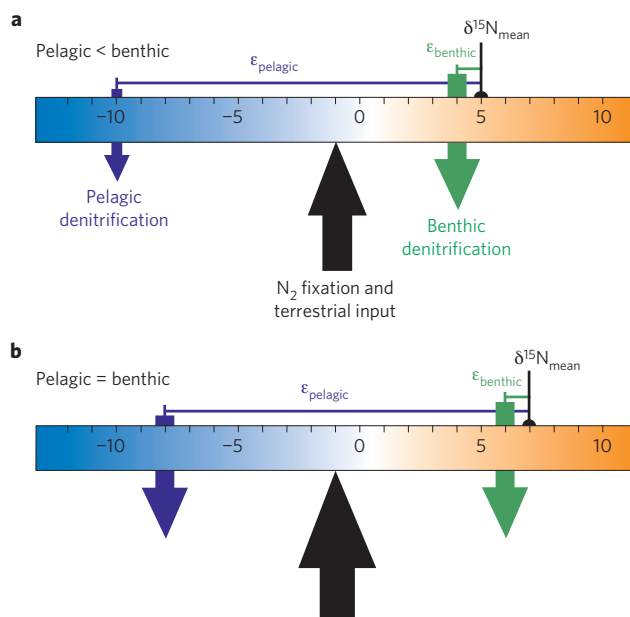[†]A full list of authors and their affiliations appears at the end of the paper

Figure 1 | The global nitrogen isotopic balance. At steady state, the two denitrification 'weights' are balanced around the 'fulcrum' of new nitrogen inputs. Pelagic denitrification strongly discriminates against ^{15}N, with an expressed fractionation factor $\varepsilon_{pelagic}$ of ~12–15‰ relative to $\delta^{15}N_{mean}$ (refs 11,42), much larger than $\varepsilon_{benthic}$ (refs 35,46,47). Because denitrification preferentially removes ^{14}N from the ocean, $\delta^{15}N_{mean}$ must be higher than the δ^{15}N of inputs (approximately −1‰, ref. 35). Insofar as the fractionation factors are fixed, any change in pelagic:benthic fluxes requires that $\delta^{15}N_{mean}$ adjust to re-establish mass balance (compare **a**,**b**).

of inventory-altering and internal-cycling processes, as expected from local studies[3,9,14].

Because ocean circulation redistributes the effects of these processes in complex ways, models of ocean physics and biogeochemistry help to illustrate the interplay between them[15] (Supplementary Information). A relatively simple model can produce isotopic gradients similar to those found in the data, through inventory-altering and internal-cycling processes (Fig. 2b,c,d). In general, inventory-altering fractionation is more significant in the tropics, where high values are generated in small areas by pelagic denitrification (solid contours, Fig. 2d) and low values by N$_2$ fixation (dashed contours, Fig. 2d). The localization arises from the confinement of suboxic waters to the tropics, and the model assumption that N$_2$ fixation occurs in warm waters[15]. Note that errors in the oxygen simulation result in denitrification occurring, incorrectly, in the SE Atlantic and Bay of Bengal, and not in the Arabian Sea, explaining most of the δ^{15}N discrepancies in these regions. Meanwhile, the effect of internal cycling is strong at all latitudes, with the greatest impact in the most nitrate-rich and nitrate-poor regions (contours, Fig. 2c). The broad distribution of the internal cycling effect may seem surprising, given the common idea of uptake and remineralization as vertical processes within the water column. However, this is a consequence of the perpetual redistribution of residual nitrate by ocean circulation, a process that is simulated well by general circulation models: fractional uptake in one region has an impact on the δ^{15}N of nitrate elsewhere, via the intervening mixing and advection of ocean waters (see also Supplementary Fig. S1).

A significant model-data discrepancy is that the simulated δ^{15}N of sinking organic matter is lower than observed (Supplementary Fig. S2). This offset agrees, both in magnitude and distribution, with the widely documented enrichment of ^{15}N due to early diagenesis in oxygenated, slowly accumulating open ocean sediments[8]. This diagenetic alteration is broadly consistent among regions, is probably caused by the preferential loss of ^{14}N during the remineralization of sedimented organic matter, and is greater in deep, well-oxygenated sediments[8]. Techniques to measure the δ^{15}N of selected compounds and of fossil-bound organic matter[16–21] are currently helping to quantify this offset, while simultaneously providing new insights on ^{15}N variability among groups of organisms in the same community[18,22,23]. Nonetheless, the bulk δ^{15}N remains a reliable sedimentary archive in most locations[13]. Given that water depth is the strongest predictor of diagenetic offset, we use a simple correction of $0.75‰\,km^{-1}$ as suggested by ref. 8 to partially mitigate the diagenetic bias, improving the model–data agreement (Supplementary Information). We apply this correction to all measurements in the analysis below.

The δ^{15}N of organic matter export across the deglaciation

Our database includes 76 records of bulk sediment δ^{15}N covering the period 30–5 kyr. Most of the records are from coastal and equatorial regions, leaving the majority of the deep sea relatively under-represented. However, as shown in Fig. 3, the good data coverage in regions with a high export flux of organic matter provides a much better constraint on the past sinking flux of δ^{15}N than might appear from the relatively sparse distribution of records in the open ocean. Furthermore, the seafloor δ^{15}N data show strong consistency between neighbouring sites[13], suggesting that the available records can be used to characterize oceanographic regions. Supported by these observations, we subdivide the ocean into δ^{15}N provinces of similar oceanographic character, guided by the distributions of pelagic denitrification, N$_2$ fixation, and nitrate-rich regions (Supplementary Information for details).

We thus define sixteen δ^{15}N provinces, each of which includes at least one sedimentary record spanning the deglaciation (Supplementary Fig. S3). Averaging the records within each province provides 16 deglacial timeseries (Supplementary Fig. S4), which show a broad range of δ^{15}N (spanning >7‰ during the Holocene). This robust spatial diversity highlights the importance of measuring a large number of δ^{15}N records to discern global processes. We use the δ^{15}N provinces to first examine qualitative changes in pelagic denitrification zones, and subsequently to calculate the deglacial history of $\delta^{15}N_{mean}$.

The deglacial history of pelagic denitrification provinces

Although it is widely thought that pelagic denitrification accelerated during the deglaciation, reports of its timing have varied[24–28]. Figure 4b shows the δ^{15}N timeseries for the four provinces where pelagic denitrification occurs today, representing a total of 20 records. Given that ocean-biogeochemical models show little impact of internal cycling fractionation in any of these four provinces (Fig. 2 and Supplementary Fig. S1) we assume, like most prior workers, that the strong local signal of pelagic denitrification was a major component of past variability therein. The δ^{15}N of the eastern Pacific provinces began increasing at ~18 kyr (refs 27–29), during Heinrich Stadial 1 (HS1), preceding the δ^{15}N rise of the Arabian Sea at ~14.5 kyr (ref. 26). Subsequently, the Pacific Ocean and Indian Ocean provinces were antiphased, such that the mean δ^{15}N of the four pelagic denitrification provinces reached a peak near 15 kyr and remained there (Fig. 4c, see Supplementary Information for further discussion).

The early deglacial response in pelagic denitrification provinces of the Pacific predated the sharp expansion of hypoxic waters within the upper ~2 km of the northern Indo-Pacific at ~14.5 kyr, the start of the Bølling–Allerød[30], but coincided with trace metal indications of decreasing oxygen at intermediate depths of the Southeast Pacific[31] and eastern tropical North Pacific[27]. This contrast seems to reflect a decoupling between the oxygenation of the eastern Pacific shadow zones and the northern Pacific thermocline. We
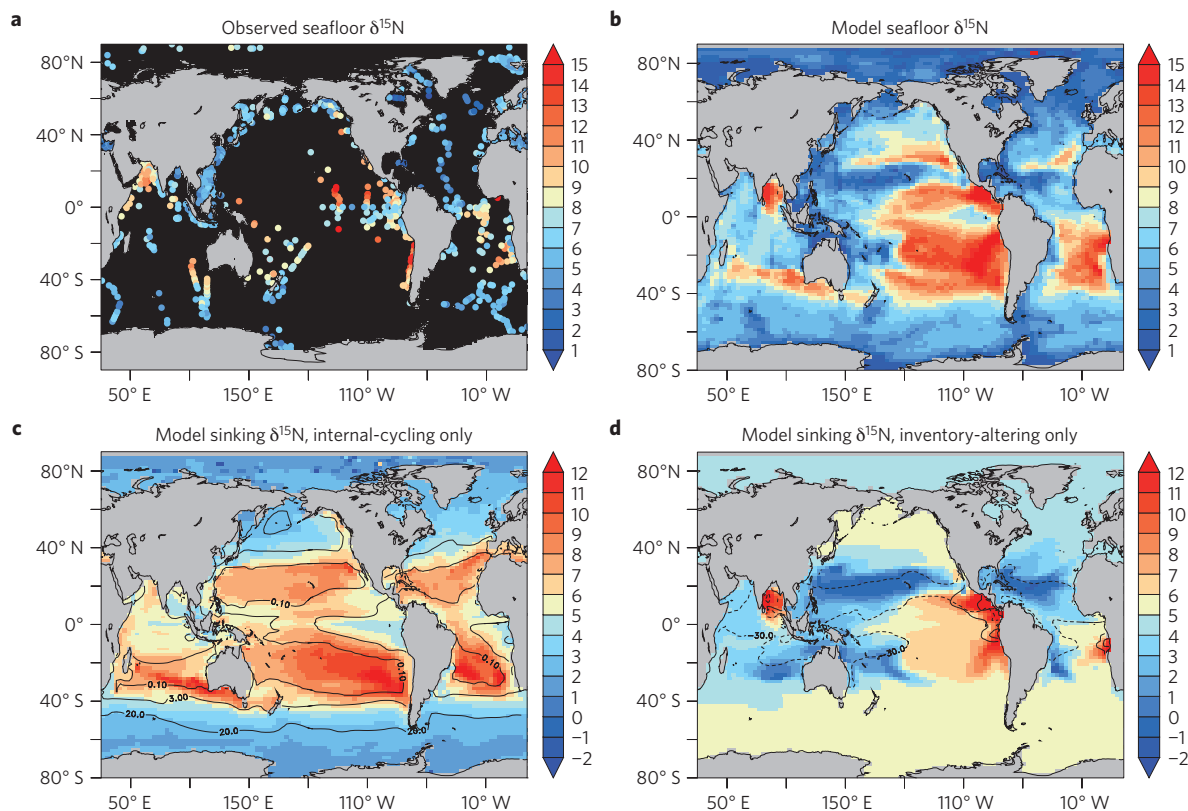
Figure 2 | The δ^{15}N of bulk sedimentary organic matter as observed and simulated. a, Observed seafloor δ^{15}N. **b**, Simulated δ^{15}N from an ocean-biogeochemistry model, with a diagenetic correction of 0.75‰ km^{-1}. **c**, Simulated δ^{15}N, including only 'internal-cycling' fractionation (shading) and modelled surface nitrate concentrations (contours, in µmol l^{-1}). See Supplementary Information for an alternative simulation. **d** as in **c**, but for only 'inventory-altering' fractionation (shading), with integrated pelagic denitrification rates (solid contours, 30 and 800 mmol N m^{-2} yr^{-1}) and N$_2$ fixation rates (dashed contours, 30 mmol N m^{-2} yr^{-1}).

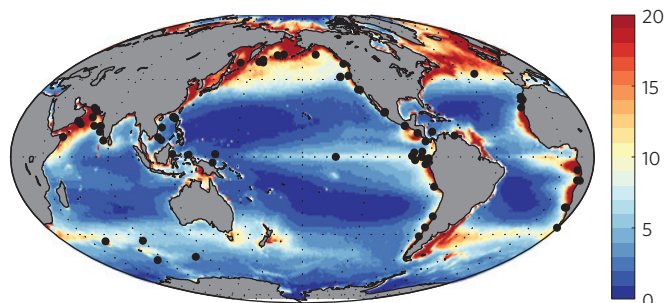**Figure 3 | Deglacial δ^{15}N records and export flux at 100 m.** Coloured shading shows export production in mmol C m^{-2} d^{-1}, according to the algorithm of ref. 48, while black circles show the locations of sediment records that have sufficient temporal resolution to be included in the deglacial analysis.

note that although the Atlantic Meridional Overturning-related mechanism of ref. 32 predicts the observed increases of hypoxic volume[30], atmospheric N$_2$O and Arabian Sea δ^{15}N during the Bølling–Allerød[30,32], it fails to predict the increase of pelagic denitrification in the Pacific during HS1. Thus, at least one additional mechanism must have fueled eastern Pacific suboxia at this time, such as ventilation of the suboxic zones, local winds[33], or changes in nutrient supply[34].

The deglacial history of ocean mean δ^{15}N

The δ^{15}N$_{mean}$ is strongly controlled by the balance of pelagic:benthic denitrification[11,35]. This property makes δ^{15}N$_{mean}$ a very useful quantity to track over time. The globally distributed δ^{15}N-province records allow us to estimate the average δ^{15}N of organic matter sinking out of the upper ocean (δ^{15}N$_{global\_export}$). We do this by weighting the δ^{15}N-province records by a satellite-derived estimate of export production within each province, to achieve a flux-weighted estimate (Supplementary Information). If the ocean were perfectly mixed in terms of nitrogen isotopes, δ^{15}N$_{global\_export}$ would be equal to δ^{15}N$_{mean}$. However, because of the heterogeneous distribution of nitrogen isotopes in the ocean, δ^{15}N$_{global\_export}$ would be expected to deviate from δ^{15}N$_{mean}$ to some degree. To explore the difference between δ^{15}N$_{global\_export}$ and δ^{15}N$_{mean}$, we used a simple two-box model of the ocean to produce a Monte Carlo estimate including a broad range of variations in denitrification, N$_2$ fixation, terrigenous N supply and nitrate utilization, and compared this to the results of simulations with ocean-biogeochemistry models (Supplementary Information). The results suggest that δ^{15}N$_{mean}$ = δ^{15}N$_{global\_export}$ + 1.0 ± 0.6‰ (1 s.d.), with the positive offset due mostly to partial nitrate consumption in the surface ocean, and the export of newly fixed nitrogen with low δ^{15}N. This offset is likely to vary over time to some degree, and deserves further study in the future, but it seems unlikely to have varied beyond our 1 s.d. bounds over the deglaciation. Finally, we vary the relative export flux accounted for by each of the δ^{15}N provinces by ±20%, to reflect uncertain variations in export production that may have arisen from changes in nutrient supply and iron fertilization (Supplementary Information).

Figure 4e shows the resulting deglacial history of δ^{15}N$_{mean}$, within a window of uncertainty calculated by the Monte Carlo assessment. Remarkably, despite the apparent acceleration of pelagic denitrification, the δ^{15}N$_{mean}$ during the Last Glacial Maximum (LGM,
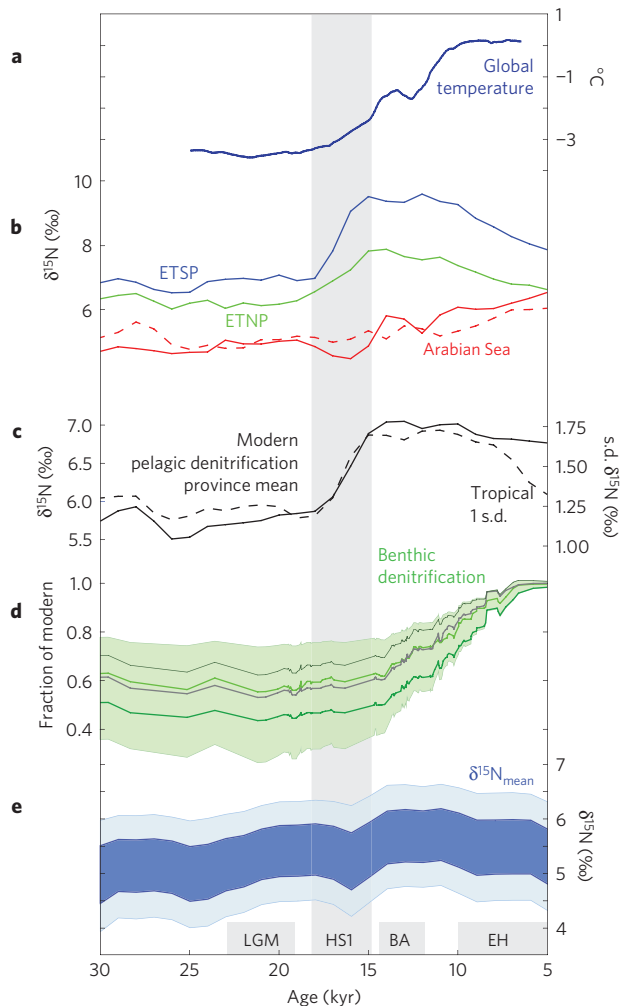
Figure 4 | Deglacial changes in denitrification and $\delta^{15}N_{mean}$.
a, Multi-proxy global temperature reconstruction[49]. **b**, Average $\delta^{15}N$ in modern pelagic denitrification regions: Eastern Tropical South Pacific (ETSP), Eastern Tropical North Pacific (ETNP) and the Arabian Sea (western, solid; eastern, dashed). **c**, Average of the four curves in **b** (solid) and standard deviation of all tropical provinces (dashed). **d**, Global benthic denitrification rate estimate, with representative error window. **e**, $\delta^{15}N_{mean}$ with shaded areas bracketing the cumulative error estimate (1 and 2 s.e.m.). The grey time intervals indicate Heinrich Stadial 1 (HS1), Last Glacial Maximum (LGM), Bølling–Allerød (BA) and Early Holocene (EH).

23–19 kyr, 5.3 ± 0.5‰) is statistically indistinguishable from that of the early Holocene (10–5 kyr, 5.4 ± 0.5‰). This result supports the suggestions of refs 11,36, based on a much smaller number of records, that the glacial–interglacial change of $\delta^{15}N_{mean}$ was small. The lack of change in $\delta^{15}N_{global\_export}$ is due to the fact that most provinces do not show a net deglacial change, while the pronounced increase of $\delta^{15}N$ in the relatively small pelagic denitrification provinces is counterbalanced by decreasing $\delta^{15}N$ in the Southern Ocean (Supplementary Information).

The lack of change in $\delta^{15}N_{mean}$ should, according to the current understanding and assuming no change in fractionation factors, reflect approximately equal pelagic:benthic global denitrification rates (Fig. 1, ref. 11). Thus, it seems that benthic and pelagic denitrification increased in approximately the same proportion between the LGM and early Holocene. This may be a coincidence, as pelagic denitrification is most sensitive to the rate of remineralization in the most poorly ventilated pockets of the ocean, whereas benthic denitrification is most sensitive to the flux of organic

matter to sediments, much of which occurs on continental shelves[37]. Although we cannot directly estimate the pelagic denitrification rates from the isotopic data, we can use a process-based algorithm to estimate how the deglacial sea-level rise[10] altered the global rate of benthic denitrification, and thereby provide an indirect quantification of the pelagic denitrification rate through the constraint that it increased proportionally.

Glacial–interglacial changes in global denitrification rates

A recent study[37] used the widely applied parameterization of ref. 38 to calculate benthic denitrification as a global, two-dimensional field, from satellite-derived export production and water depth. Given that the deglacial history of eustatic sea level is reasonably well known[39], we recalculate benthic denitrification using four different algorithms and the transient sea-level history over the past 30 kyr (Supplementary Information). The results indicate that benthic denitrification changed very little between 30 and 15 kyr, and then increased by ~30–120% between 15 and 8 kyr to modern rates (Fig. 4d). The relatively late acceleration of benthic denitrification is due to the large fraction of continental shelves at depths <80 m below modern sea level. We caution that this estimate arises from the benthic denitrification parameterizations, and assumes that the total export flux of organic carbon during the LGM did not significantly exceed the present flux, consistent with other studies[40,41]; the estimate should be updated in the future as further information becomes available.

Our isotopic constraint therefore implies that pelagic denitrification increased by an amount similar to the ~30–120% increase of benthic denitrification. Given the modern residence time for N_{bio} of ~3 kyr (ref. 1) and the apparent stability of the glacial and Holocene intervals, the N cycle must have been close to balanced throughout each interval[11,42]. Thus, it follows that N_2 fixation also increased by ~30–120% between the LGM and mid-Holocene, qualitatively in accord with individual $\delta^{15}N$ records from hotspots of N_2 fixation[18]. Low glacial rates of N_2 fixation, relative to today, could have arisen from the reduced ecological competitiveness of diazotrophs, given a relatively high-N:P surface ocean[43] and/or low p_{CO_2} (ref. 44), despite the greater dust-borne supply of iron.

Although the nitrogen cycle seems to have approached steady state during the LGM and Holocene, a significant change in the inventory of N_{bio} may have occurred during the deglacial transient. While the loss of N_{bio} was accelerating, the welfare of diazotrophs was being driven in opposite directions by the boon of rising p_{CO_2} (ref. 44) and the harsher iron limitation caused by dwindling of the glacial dust supply[4,45]. The $\delta^{15}N_{mean}$ shows a small maximum during the late deglaciation, as expected from a lag of benthic denitrification and N_2 fixation[18] relative to pelagic denitrification, which may have caused a decrease of the N inventory as discussed in detail in ref. 11 (Fig. 4e). We note that our steady-state approximation of $\delta^{15}N_{mean}$ from $\delta^{15}N_{global\_export}$ is less appropriate during the deglacial transient and it is therefore possible that $\delta^{15}N_{mean}$ changed by more than implied by Fig. 4e.

In summary, this analysijs has confirmed that the $\delta^{15}N$ of seafloor sediment provides a robust record of past changes in the nitrogen cycle, and has constrained how the inventory fluxes of N_{bio} increased in response to deglacial climate warming. There is a clear need to improve the spatial coverage of $\delta^{15}N$ records, given the importance of a global dataset for constraining past changes, and to measure mineral-bound, compound-specific or other N pools wherever bulk $\delta^{15}N$ is problematic[18]. In particular, the Southern Ocean and North Atlantic, which together account for 30% of the global export, are under-represented. Meanwhile, stronger constraints on the isotopic effects, better process models of benthic denitrification, and independent measures of deep ocean $\delta^{15}N$ and export production fluxes will reduce the quantitative

uncertainties. Finally, extending the global record of nitrogen isotopes further back in time will help to constrain the relationships between climate and the nitrogen cycle under a broader range of environmental conditions.

Methods

The NICOPP database is available at http://www.ncdc.noaa.gov/paleo/pubs/nicopp/nicopp.html.

References

1. Gruber, N. & Galloway, J. N. An Earth-system perspective of the global nitrogen cycle. *Nature* **451,** 293–296 (2008).
2. Ravishankara, A. R., Daniel, J. S. & Portmann, R. W. Nitrous oxide (N_2O): The dominant ozone-depleting substance emitted in the 21st century. *Science* **326,** 123–125 (2009).
3. Ganeshram, R. S., Pedersen, T. F., Calvert, S. E. & Murray, J. W. Large changes in oceanic nutrient inventories from glacial to interglacial periods. *Nature* **376,** 755–758 (1995).
4. Falkowski, P. G. Evolution of the nitrogen cycle and its influence on the biological sequestration of CO_2 in the ocean. *Nature* **387,** 272–275 (1997).
5. Schmittner, A., Oschlies, A., Matthews, H. D. & Galbraith, E. D. Future changes in climate, ocean circulation, ecosystems, and biogeochemical cycling simulated for a business-as-usual CO_2 emission scenario until year 4000 AD. *Glob. Biogeochem. Cycl.* **22,** http://dx.doi.org/10.1029/2007gb002953 (2008).
6. Sarmiento, J. L., Hughes, T. M. C., Stouffer, R. J. & Manabe, S. Simulated response of the ocean carbon cycle to anthropogenic climate warming. *Nature* **393,** 245–249 (1998).
7. Deutsch, C., Brix, H., Ito, T., Frenzel, H. & Thompson, L. Climate-forced variability of ocean hypoxia. *Science* **333,** 336–339 (2011).
8. Robinson, R. S. *et al.* A review of nitrogen isotopic alteration in marine sediments. *Paleoceanography* **27** (2012).
9. Altabet, M. A., Francois, R., Murray, D. W. & Prell, W. L. Climate-related variations in denitrification in the arabian sea from sediment $^{15}N/^{14}N$ ratios. *Nature* **373,** 506–509 (1995).
10. Christensen, J. J., Murray, J. W., Devol, A. H. & Codispoti, L. A. Denitrification in continental shelf sediments has major impact on the oceanic nitrogen budget. *Glob. Biogeochem. Cycl.* **1,** 97–116 (1987).
11. Deutsch, C., Sigman, D. M., Thunell, R. C., Meckler, A. N. & Haug, G. H. Isotopic constraints on glacial/interglacial changes in the oceanic nitrogen budget. *Glob. Biogeochem. Cycl.* **18,** http://dx.doi.org/10.1029/2003GB002189 (2004).
12. Altabet, M. A. *et al.* The nitrogen isotope biogeochemistry of sinking particles from the margin of the Eastern North Pacific. *Deep-Sea Res. I* **46,** 655–679 (1999).
13. Tesdal, J., Galbraith, E. D. & Kienast, M. Nitrogen isotopes in bulk marine sediment: linking seafloor observations with subseafloor records. *Biogeosciences* **10,** 101–118 (2013).
14. Altabet, M. A. & Francois, R. Sedimentary nitrogen isotopic ratio as a recorder for surface ocean nitrate utilization. *Glob. Biogeochem. Cycl.* **8,** 103–116 (1994).
15. Somes, C. J. *et al.* Simulating the global distribution of nitrogen isotopes in the ocean. *Glob. Biogeochem. Cycl.* **24,** http://dx.doi.org/10.1029/2009gb003767 (2010).
16. McCarthy, M. D., Benner, R., Lee, C. & Fogel, M. L. Amino acid nitrogen isotopic fractionation patterns as indicators of heterotrophy in plankton, particulate, and dissolved organic matter. *Geochim. Cosmochim. Acta* **71,** 4727–4744 (2007).
17. Robinson, R. S. *et al.* Diatom-bound N-15/N-14: New support for enhanced nutrient consumption in the ice age subantarctic. *Paleoceanography* **20,** http://dx.doi.org/10.1029/2004PA001114 (2005).
18. Ren, H. *et al.* Foraminiferal isotope evidence of reduced nitrogen fixation in the ice age atlantic ocean. *Science* **323,** 244–248 (2009).
19. Mobius, J., Gaye, B., Lahajnar, N., Bahlmann, E. & Emeis, K. C. Influence of diagenesis on sedimentary delta(15)N in the Arabian Sea over the last 130 kyr. *Mar. Geol.* **284,** 127–138 (2011).
20. Sherwood, O. A., Lehmann, M. F., Schubert, C. J., Scott, D. B. & McCarthy, M. D. Nutrient regime shift in the western North Atlantic indicated by compound-specific delta(15)N of deep-sea gorgonian corals. *Proc. Natl Acad. Sci. USA* **108,** 1011–1015 (2011).
21. Higgins, M. B., Robinson, R. S., Carter, S. J. & Pearson, A. Evidence from chlorin nitrogen isotopes for alternating nutrient regimes in the Eastern Mediterranean Sea. *Earth Planet. Sci. Lett.* **290,** 102–107 (2010).
22. Brunelle, B. G. *et al.* Evidence from diatom-bound nitrogen isotopes for Subarctic Pacific stratification during the last ice age and a

23. link to North Pacific denitrification changes. *Paleoceanography* **22,** http://dx.doi.org/10.1029/2005PA001205 (2007).
23. Horn, M. G., Robinson, R. S., Rynearson, T. A. & Sigman, D. M. Nitrogen isotopic relationship between diatom-bound and bulk organic matter of cultured polar diatoms. *Paleoceanography* **26,** http://dx.doi.org/10.1029/2010pa002080 (2011).
24. Pride, C. *et al.* Nitrogen isotopic variations in the Gulf of California since the last deglaciation: Response to global climate change. *Paleoceanography* **14,** 397–409 (1999).
25. Emmer, E. & Thunell, R. C. Nitrogen isotope variations in Santa Barbara Basin sediments: Implications for denitrification in the eastern tropical North Pacific during the last 50,000 years. *Paleoceanography* **15,** 377–387 (2000).
26. Suthhof, A., Ittekkot, V. & Gaye-Haake, B. Millennial-scale oscillation of denitrification intensity in the Arabian Sea during the late Quaternary and its potential influence on atmospheric N2O and global climate. *Glob. Biogeochem. Cycl.* **15,** 637–649 (2001).
27. Hendy, I. L. & Pedersen, T. F. Oxygen minimum zone expansion in the eastern tropical North Pacific during deglaciation. *Geophys. Res. Lett.* **33,** http://dx.doi.org/10.1029/2006GL025975 (2006).
28. De Pol-Holz, R. *et al.* Melting of the Patagonian Ice Sheet and deglacial perturbations of the nitrogen cycle in the eastern South Pacific. *Geophys. Res. Lett.* **33,** http://dx.doi.org/10.1029/2006GL025975 (2006).
29. Robinson, R., Mix, A. & Martinez, P. Southern Ocean control on the extent of denitrification in the southeast Pacific over the last 70 ky. *Quat. Sci. Rev.* **26,** 201–212 (2007).
30. Jaccard, S. L. & Galbraith, E. D. Large climate-driven changes of oceanic oxygen concentrations during the last deglaciataion. *Nature Geosci.* **5,** 151–156 (2012).
31. Muratli, J. M., Chase, Z., Mix, A. C. & McManus, J. Increased glacial-age ventilation of the Chilean margin by Antarctic Intermediate Water. *Nature Geosci.* **3,** 23–26 (2010).
32. Schmittner, A. & Galbraith, E. D. Glacial greenhouse-gas fluctuations controlled by ocean circulation changes. *Nature* **456,** 373–376 (2008).
33. Kienast, M. *et al.* Eastern Pacific cooling and Atlantic overturning circulation during the last deglaciation. *Nature* **443,** 846–849 (2006).
34. Martinez, P. & Robinson, R. S. Increase in water column denitrification during the last deglaciation: The influence of oxygen demand in the eastern equatorial Pacific. *Biogeosciences* **7,** 1–9 (2010).
35. Brandes, J. A. & Devol, A. H. A global marine-fixed nitrogen isotopic budget: Implications for Holocene nitrogen cycling. *Glob. Biogeochem. Cycl.* **16,** http://dx.doi.org/10.1029/2001GB001856 (2002).
36. Kienast, M. Unchanged nitrogen isotopic composition of organic matter in the South China Sea during the last climatic cycle: Global implications. *Paleoceanography* **15,** 244–253 (2000).
37. Bianchi, D., Dunne, J. P., Sarmiento, J. L. & Galbraith, E. D. Data-based estimates of suboxia, denitrification, and N2O production in the ocean and their sensitivities to dissolved O-2. *Glob. Biogeochem. Cycl.* **26,** http://dx.doi.org/10.1029/2011gb004209 (2012).
38. Middelburg, J. J., Soetaert, K., Herman, P. M. J. & Heip, C. H. R. Denitrification in marine sediments: A model study. *Glob. Biogeochem. Cycl.* **10,** 661–673 (1996).
39. Clark, P. U. *et al.* The last glacial maximum. *Science* **325,** 710–714 (2009).
40. Oka, A., Abe-Ouchi, A., Chikamoto, M. O. & Ide, T. Mechanisms controlling export production at the LGM: Effects of changes in oceanic physical fields and atmospheric dust deposition. *Global Biochemical Cycles* **25,** http://dx.doi.org/10.1029/2009GB003628 (2011).
41. Kohfeld, K., Le Quéré, C., Harrison, S. P. & Anderson, R. F. Role of marine biology in glacial–interglacial CO_2 cycles. *Science* **308,** 74–78 (2005).
42. Altabet, M. A. Constraints on oceanic N balance/imbalance from sedimentary ^{15}N records. *Biogeosciences* **4,** 75–86 (2007).
43. Tyrrell, T. The relative influences of nitrogen and phosphorus on oceanic primary production. *Nature* **400,** 525–531 (1999).
44. Hutchins, D. A. *et al.* CO_2 control of Trichodesmium N_2 fixation, photosynthesis, growth rates, and elemental ratios: Implications for past, present, and future ocean biogeochemistry. *Limnol. Oceanogr.* **52,** 1293–1304 (2007).
45. Eugster, O., Gruber, N., Deutsch, C., Jaccard, S. L. & Payne, M. R. The dynamics of the marine nitrogen cycle across the last deglaciation. *Paleoceanography* **28,** 1–14 (2013).
46. Lehmann, M. F. *et al.* The distribution of nitrate $^{15}N/^{14}N$ in marine sediments and the impact of benthic nitrogen loss on the isotopic composition of oceanic nitrate. *Geochim. Cosmochim. Acta* **71,** 5384–5404 (2007).
47. Lehmann, M. F., Sigman, D. M. & Berelson, W. M. Coupling the $^{15}N/^{14}N$ and $^{18}O/^{16}O$ of nitrate as a constraint on benthic nitrogen cycling. *Mar. Chem.* **88,** 1–20 (2004).
48. Dunne, J. P., Sarmiento, J. L. & Gnanadesikan, A. A synthesis of global particle export from the surface ocean and cycling through the ocean interior and on the seafloor. *Glob. Biogeochem. Cycl.* **21,** http://dx.doi.org/10.1029/2006gb002907 (2007).

49. Shakun, J. D. *et al.* Global warming preceded by increasing carbon dioxide concentrations during the last deglaciation. *Nature* **484,** 49–55 (2012).

Author contributions

M.K., T.K. and E.D.G. initiated and led the NICOPP working group. J-E.T., E.D.G. and M.K. assembled the database. D.B. made the δ^{15}N-province, benthic denitrification and box model calculations. C.S. ran the UVic biogeochemical model simulations. E.D.G. wrote the manuscript with contributions from M.K. All coauthors participated in discussions at the working group meetings and edited the manuscript, and/or contributed previously unpublished data.

Additional information

Supplementary information is available in the online version of the paper. Reprints and permissions information is available online at www.nature.com/reprints. Correspondence and requests for materials should be addressed to E.G.

Competing financial interests

The author declares no competing financial interests.

Eric D. Galbraith[1]*, Markus Kienast[2], Ana Luiza Albuquerque[3], Mark A. Altabet[4], Fabian Batista[5], Daniele Bianchi[1], Stephen E. Calvert[6], Sergio Contreras Quintana[7], Xavier Crosta[8], Ricardo De Pol Holz[9], Nathalie Dubois[10], Johan Etourneau[11], Roger Francois[6], Ting-Chang Hsu[12], Tara Ivanochko[6], Samuel Jaccard[13], Shuh-Ji Kao[14], Thorsten Kiefer[15], Stephanie Kienast[2], Moritz F. Lehmann[16], Philippe Martinez[8], Matthew McCarthy[5], Anna Nele Meckler[13], Alan Mix[17], Jürgen Möbius[18], Tom F. Pedersen[19], Laetitia Pichevin[20], Tracy M. Quan[21], Rebecca S. Robinson[22], Evgeniya Ryabenko[23], Andreas Schmittner[17], Ralph Schneider[24], Aya Schneider-Mor[25], Masahito Shigemitsu[26], Dan Sinclair[27], Christopher Somes[2], Anja S. Studer[13], Jan-Erik Tesdal[28], Robert Thunell[29] and Jin-Yu Yang[30]

[1]Department of Earth and Planetary Science, McGill University, 3450 University Street, Montreal, Quebec H3A 2A7, Canada, [2]Department of Oceanography, Dalhousie University, 1355 Oxford Street, PO Box 15000, Halifax, Nova Scotia, B3H 4R2, Canada, [3]Departamento de Geoquímica, Instituto de Química, Universidade Federal Fluminense, Rio de Janeiro, Brazil, [4]School for Marine Science and Technology, U Massachusetts Dartmouth, 706 Rodney French Blvd, Massachusetts 02744-1221, New Bedford, USA, [5]Ocean Sciences Deptartment, University of California, Santa Cruz 95064, USA, [6]Department of Earth Ocean and Atmospheric Sciences, University of British Columbia, 2020-2207 Main Mall, British Columbia, V6T 1Z4, Canada, [7]Large Lakes Observatory, University of Minnesota Duluth, 2205 E. 5th Street, Research Laboratory Building 205, Duluth, Minnesota 55812, USA, [8]Université Bordeaux 1, UMR CNRS 5805 EPOC, Avenue des facultés, 33405 Talence cedex, France, [9]Department of Oceanography, Center for Climate and Resilience Research (CR)², Universidad de Concepció, Casilla 160-C, Concepcion, Chile, [10]Woods Hole Oceanographic Institution, Clark 120A, MS #23, Woods Hole, Massachusetts 02543, USA, [11]UMR 7159 LOCEAN, Université Pierre et Marie Curie, Institut Pierre Simon Laplace, 4 Place Jussieu, Boite 100, 75252 Paris Cedex 05, France, [12]Research Center for Environmental Changes, Academia Sinica, 128 Academia Road, Sec. 2, Nankang Taipei, Taiwan, R.O.C., [13]Geological Institute, ETH Zurich, Sonneggstrasse 5, CH-8092 Zurich, Switzerland, [14]Research Center for Environmental Changes, Academia Sinica, Taipei, Taiwan, [15]PAGES International Project Office, Zähringerstrasse 25, 3012 Bern, Switzerland, [16]Department of Environmental Sciences, University of Basel, Bernoullistrasse 30, CH-4056 Basel, Switzerland, [17]College of Earth, Oceanic, & Atmospheric Sciences, Oregon State University, CEOAS Administration Building 104, Corvallis, Oregon 97331-5503, USA, [18]Institute for Biogeochemistry and Marine Chemistry, Hamburg University, Bundesstrasse 55, 20146 Hamburg, Germany, [19]Pacific Institute for Climate Solutions, University of Victoria, PO Box 1700 STN CSC, Victoria, British Columbia, V8W 2Y2, Canada, [20]School of Geosciences, The University of Edinburgh, West Mains Road, Edinburgh EH9 3JW, Scotland, UK, [21]Boone Pickens School of Geology, Oklahoma State University, 105 Noble Research Center, Stillwater, Oklahoma 74074, USA, [22]Graduate School of Oceanography, University of Rhode Island, Narragansett Bay Campus, Narragansett, Rhode Island 02882, USA, [23]GEOMAR Helmholtz-Centre for Ocean Research Kiel, Düsternbrooker Weg 20, 24105 Kiel, Germany, [24]Institut fuer Geowissenschaften, Christian-Albrechts-Universitaet zu Kiel, Ludewig-Meyn-Str. 10, 24118 Kiel, Germany, [25]Department of Geological and Environmental Sciences, Stanford University, 367 Panama Street, California 94305, Stanford, USA, [26]Faculty of Environmental Earth Science, Hokkaido University, Sapporo, Japan, [27]Institute of Marine and Coastal Sciences, Rutgers University, Newark, 71 Dudley Road, New Brunswick, New Jersey 08901-8525, USA, [28]School of Earth and Ocean Sciences, University of Victoria, 3800 Finnerty Road (Ring Road), PO Box 1700 Station CSC, Victoria, British Columbia, V8W 2Y2, Canada, [29]Department of Earth and Ocean Sciences, University of South Carolina, Columbia, South Carolina 29208, USA, [30]State Key Laboratory of Marine Environmental Science, Xiamen University, Xiamen, China. *e-mail: eric.galbraith@mcgill.ca.

Page 1